

Mapping and Assessment of Within-Field Spatial Variability of Soil pH, Electrical Conductivity, and Particle Size Distribution to Delineate Management Zones

Marcial S. Buladaco II^{1*}, Hannah Mae F. Tandugon¹, Michelle Anne B. Bunquin¹, Pearl B. Sanchez¹, Sophia Alelie C. Bugia¹, Nicole Ann P. Yales¹, Sarah M. Casacop¹

¹ Division of Soil Science, Agricultural Systems Institute, College of Agriculture and Food Science, University of the Philippines Los Baños, College, Laguna, Philippines

* Corresponding author's e-mail: msbuladaco@up.edu.ph

ABSTRACT

The study aimed to evaluate the spatial distribution of soil pH, electrical conductivity (EC), and particle size distribution within a seven-hectare field in Los Baños Laguna, Philippines using the ordinary kriging method and to utilize the interpolated maps to delineate management zones. Fifty soil samples were collected from the surface layer at a depth of 0–20 cm using a random sampling technique. On the basis of the obtained results, it was found that the area has an acidic pH, medium-textured soil with low soluble salt content. Geostatistical analysis revealed that soil EC and clay content exhibited strong spatial dependence, while soil pH and silt were observed to have a moderate spatial dependence. In contrast, sand exhibited weak spatial dependence. The spherical model was identified as the optimal fit for soil pH, clay content, silt content, and sand content, while the exponential model was deemed most suitable for EC. Three distinct management zones (MZs) were delineated based on the spatial variability of the selected properties. MZ1, the largest zone covering 82.10% of the area, is characterized by a weakly acidic, clay loam soil while MZ2, comprising 15.11% of the area, has a weakly acidic loam soil. MZ3, the smallest zone occupying 2.79% of the area, has a highly acidic loam soil and may require frequent as well as intensive lime applications. These findings highlight the varied spatial dependency and distribution of soil characteristics even in a relatively small area and the usefulness of the interpolated maps as a valuable tool to identify specific management zones.

Keywords: electrical conductivity, geostatistics, management zones, particle size distribution, soil pH.

INTRODUCTION

The management zone (MZ) approach is a field-specific strategy that divides the field into smaller zones based on shared limitations to crop yield [Vrindts et al., 2005], depending on the comparable environmental conditions. Significant and relevant parameters are those that directly influence crop yield, including - but not limited to - soil properties like soil pH, moisture condition, OM, and texture. Researchers and practitioners combine various parameters to delineate management zones. Delineating MZs involves utilizing various data points derived from crop yield maps [Santi et al., 2013; Damian et al., 2017], farmer's

knowledge [Koch et al., 2004; Heijting et al., 2011], geomorphology [Nolan et al. 2000, Fraisse et al., 2001], remotely sensed data [Georgi et al., 2018; Jin et al., 2017], and soil properties [Gili et al., 2017; Tripathi et al., 2015].

Understanding the field-specific soil properties within an area is an effective tool for sustainable resource management [AbdelRahman et al., 2021]. Significant variation in the complexity of the soil properties over both larger regional areas and smaller field scales is observed, exhibiting diverse spatial and temporal patterns, even within soil series or mapping units [Amirinejad et al., 2011; Laekemariam et al., 2018; Shukla et al., 2016]. Due to the dynamic effects of soil

processes influenced by the elements of soil formation and by extrinsic variables, such as cropping patterns, application of agricultural inputs, and management practices, among others, soil properties vary throughout regions [Buol et al., 2011; Liu et al., 2015; Shi et al., 2009].

Accurate spatial variability characterization requires methods beyond the traditional soil collection and laboratory analysis, as these methods remain uneconomical when dealing with large volumes of soil. Spatial interpolation is a process of using known points with available observed data to estimate values at other unknown points [Losser et al., 2014]. It includes deterministic and geostatistical interpolation methods. While various geostatistical methods exist for assessing soil heterogeneity, kriging is the commonly preferred method utilized by researchers [Desavathu et al., 2017; Reza et al., 2016; Vasu et al., 2017]. Various kriging approaches include disjunctive, indicator, ordinary, simple, and universal kriging methods. Ordinary kriging, a commonly trusted and extensively used method, operates on the assumption that the mean value is constant but unknown. Researchers have extensively employed this method to spatially map various soil characteristics [Li et al., 2013; Yang et al., 2012].

The within-field spatial variability of various soil characteristics has gained significant focus in recent decades [Leroux and Tisseyre, 2019]. The studies commonly pertain to the homogeneity and heterogeneity of the areas within a field as well as how these similarities and differences within the field affect crop productivity [Sadras and

Bongiovanni, 2004]. In this regard, the location-specific characteristics of the area were mapped depending on the variables of interest. Most studies further assessed the specific properties within-field for site-specific management [Junior et al., 2006; Reza et al., 2010; Vasu et al., 2017] or mapping purposes [Davatgar et al., 2012; Moral et al., 2010; Xin-Zhong et al., 2009].

The spatial representation of within-field variability can be simplified through the delineation of zones within the field. The idea is to create a manageable number of uniform zones within a field to consider the key variations in soil properties that might exist across the area. Thus, this study assessed the within-field spatial distribution of soil pH, EC, and particle size distribution in a seven-hectare field using ordinary kriging and utilization of interpolated maps to delineate management zones.

MATERIAL AND METHODS

Study area

The study site is a recently established experimental research station at the University of the Philippines Los Baños, between 14.1472° N, and 121.2613° E near Bay, Laguna (Fig. 1). The area sits at an elevation of roughly 28 meters above sea level (m asl). The study area is a 7-hectare parcel of land recently developed to advance the study of short-term and long-term organic agriculture research and capability-building programs. In the

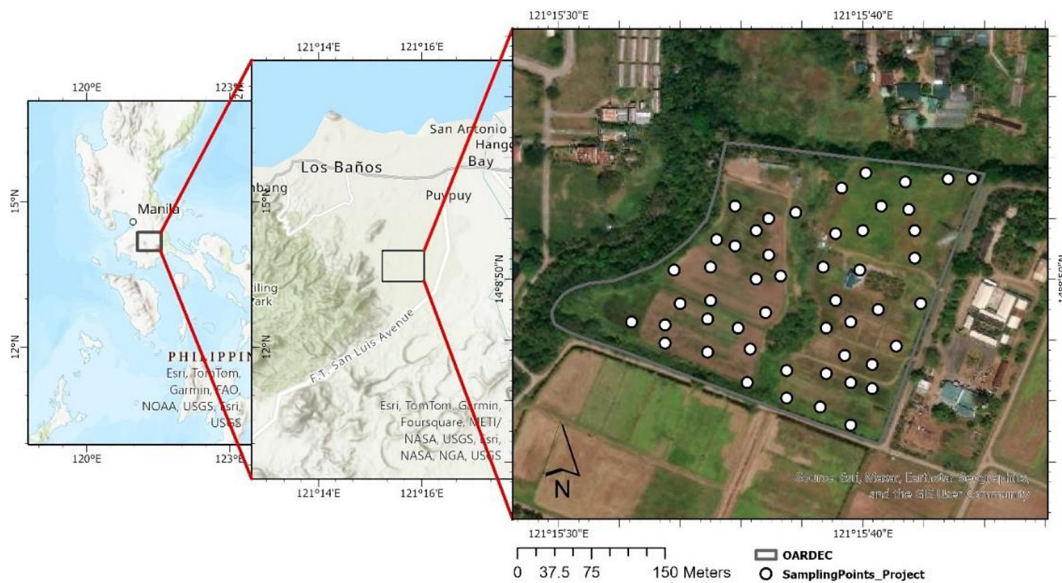


Figure 1. Location and sampling point distribution within the study area (n = 50)

past, the land was mainly used for grazing livestock. However, in 2018, it was repurposed into a research center focused on organic farming. The conversion signifies a dedication to studying and promoting organic farming methods, including experiments, data collection, as well as sharing knowledge on techniques such as crop rotation, composting, and pest control. This change from grazing land to an organic research center marks a substantial shift towards sustainable, environmentally friendly farming practices and scientific advancement in agriculture.

Soil collection and analyses

Fifty soil samples were collected from the surface layer at a depth of 0–20 cm using a random sampling technique. For each sampling point, five subsamples were combined into one large composite sample. The collected soil samples were air-dried, crushed into smaller particles, sifted through a 2-mm sieve, and stored in labeled sampling bags. Standard laboratory tests were used to analyze soil pH, in 1:5 (m:v) soil suspension in 0.01 M CaCl₂ solution [FAOb, 2021], EC, in 1:5 ratio [FAOa, 2021], and particle size distribution (hydrometer method). The textural classes were identified using the multi-point texture triangle Excel tool developed by the USDA.

Descriptive statistics and data transformation

To summarize the data, measures of central tendency (mean), spread (minimum, maximum, and standard deviation), and variability (coefficient of variation, skewness, and kurtosis) were calculated. The Kolmogorov-Smirnov (KS) test was employed to evaluate data normality. For the data that did not follow a normal distribution, the Box-Cox transformation was applied [Delbari et al., 2019; Fu et al., 2010; Pereira et al., 2017]. The relationship between the parameters was assessed using the Pearson correlation matrix. Statistical tests were performed using the Minitab® 21.3.1 statistical software.

Geostatistical analysis

The study used the geostatistical analyst GUI (ArcGIS Pro version 2.7). The kriging process follows the Equation below [Webster and Oliver, 2007].

$$Z^*(S_o) = \sum_{i=1}^N \gamma_i Z(S_i) \quad (1)$$

where: $Z^*(S_o)$ is the interpolated value at an unsampled site S_o , $Z(S_i)$ is the known value for the test parameter at the sampling location S_i , N is the site density in the search location for the interpolation, and γ_i is the weight of the determined value at S_i .

Employing various models, semivariograms were utilized to map the spatial distribution of soil properties. To determine the interpolation function, semivariogram analysis was performed as follows:

$$\gamma(h) = \frac{1}{2N(h)} \sum_{i=1}^{N(h)} (Z(S_i) - Z(S_i + h))^2 \quad (2)$$

where: $\gamma(h)$ is the spatial dependence at lag distance h , $N(h)$ is the number of sample point pairs as separated by h , and $Z(S_i)$ is the variable Z value at the location S_i .

Choosing the appropriate semivariogram model and its parameters is crucial for achieving precise interpolation [Oliver and Webster, 2014; Pardo-Igúzquiza and Dowd, 2013]. The study assessed the performance of three commonly used semivariogram functions – Gaussian (Equation 3), exponential (Equation 4), and spherical (Equation 5) – in the identification of the best-fit model that represents spatial variability within the data set. The Gaussian model demonstrates that spatial autocorrelation initially rises with increasing distance, then progressively declines, ultimately reaching zero after a particular threshold distance is surpassed. The exponential model demonstrates that spatial autocorrelation diminishes exponentially as distance increases, and autocorrelation will only cease entirely at an infinite distance. The spherical model shows that spatial autocorrelation between data points progressively weakens with increasing distance, where there is no spatial dependence at zero at a specific threshold distance.

$$\gamma(h) = C_0 + C_1 \left[1 - \exp\left(-\frac{h^2}{a^2}\right) \right] \quad h > 0 \quad (3)$$

$$\gamma(h) = C_0 + C_1 \left[1 - \exp\left(-\frac{h}{a}\right) \right] \quad h \geq 0 \quad (4)$$

$$\gamma(h) = \begin{cases} C_0 + C_1 \left[\frac{3h}{2a} - \frac{1}{2} \left(\frac{h^3}{a^3} \right) \right] & 0 < h \leq a \\ C_0 + C_1 & h > a \\ 0 & h = 0 \end{cases} \quad (5)$$

where: C_0 is the nugget, C_1 is the partial sill, $C_0 + C_1$ is the sill, and a is the range to reach sill.

Sill represents the semivariance value at which the model reaches a plateau or maximum variability that can be explained by spatial dependence, whereas the nugget represents any

variability that exists due to random factor or microscale variation (y-intercept of the semivariogram model) that cannot be attributed to spatial dependence. When the separation distance (h) is zero, the semivariogram should theoretically be zero. However, if there is a departure from this (known as the nugget effect), it might be from minor variations at a small scale or measurement errors. The range indicates the distance wherein the semivariance achieves its peak value.

Furthermore, the analysis involved calculating the nugget-to-sill ratio or degree of spatial dependence (DSD). A ratio below 25% suggests a strong spatial dependence, meaning the data points close together tend to have similar values. This dependence likely arises from inherent or internal factors influencing the variable across the study area. Conversely, a ratio above 75% indicates a weak spatial dependence, where data points have little to no correlation with distance. This suggests the existence of external factors affecting the variation. A DSD range of 25–75% indicates a moderate spatial dependence, reflecting the influence of both internal and external factors on the observed variability [Cambardella et al., 1994]. A DSD value approaching 0% signifies a significant geographic autocorrelation in the variable, but a value nearing 100% implies that the field-specific variation is mostly influenced by the nugget effect or randomness [He et al., 2010].

Cross-validation

Cross-validation is a widely used technique to check how well interpolation methods perform. This evaluation considered several parameters, including average standard error (ASE), mean error (ME), mean square error (MSE), root mean square error (RMSE), and standardized root mean square error (RMSSE).

Identification of management zones

The interpolated maps were categorized into consistent classes to define the management

zones. Soil texture was reclassified based on USDA soil textural classes while the soil $\text{pH}_{\text{CaCl}_2}$ and EC were reclassified into 5 categories according to Jones [2001] and Richards [1954], respectively. Using the ArcGIS Pro spatial analyst tool, a weighted overlay analysis was employed to generate the MZ maps.

RESULTS AND DISCUSSION

Descriptive statistics

The summary statistics of soil pH, EC, and particle size fractions are presented in Table 1. The site is generally acidic with an average pH of 4.77, ranging from 4.20 to 5.80. EC has a mean of $65.36 \mu\text{S}\cdot\text{cm}^{-1}$ and it ranges between 36.58 to $156.00 \mu\text{S}\cdot\text{cm}^{-1}$. The mean values of the particle size fractions are approximately 28.45% sand, 40.50% silt, and 31.06% clay. On the basis of the USDA texture classes, 40 samples were classified as clay loam, 9 were loam, and 1 was silt loam (Figure 2). It conforms to the fact that the area is mapped under Lipa soil series, a medium textured soil with a texture class from loam to clay loam [Carating et al., 2014]. Low standard deviation values of the soil properties were observed, except for EC. It indicates that pH and particle size fractions values are clustered around the mean value while the EC values are more spread out.

As a measure of variability, the coefficient of variation (CV) was generated describing values less than 15% as low variation, values between 15% and 35% as medium variation, and values exceeding 35% were considered high variation, as proposed by Wilding [1985]. A low CV value of 7.80% was observed in soil pH, which indicates a uniform condition in the area, which may be attributed to the minimal changes in the physiographic features, such as elevation, slope, and soil type. In contrast, EC has high variability (38.89%) indicating heterogeneity. This agrees with the findings by Khan et al. [2021]. Furthermore, low CV values were also observed for sand,

Table 1. Summary statistics of the soil properties (n = 50)

Parameter	Minimum	Maximum	Mean	SD	CV%	Skewness	Kurtosis	K-S p
$\text{pH}_{\text{CaCl}_2}$	4.20	5.80	4.77	0.37	7.80	0.50	0.02	0.115
EC, $\mu\text{S}\cdot\text{cm}^{-1}$	36.58	156.00	65.36	25.42	38.89	1.44	2.33	<0.010
Sand, %	20.18	36.42	28.45	4.03	14.17	-0.01	-0.85	>0.150
Silt, %	33.11	50.15	40.50	4.65	11.49	0.21	-0.88	>0.150
Clay, %	21.47	39.18	31.06	3.88	12.49	-0.36	-0.05	>.100

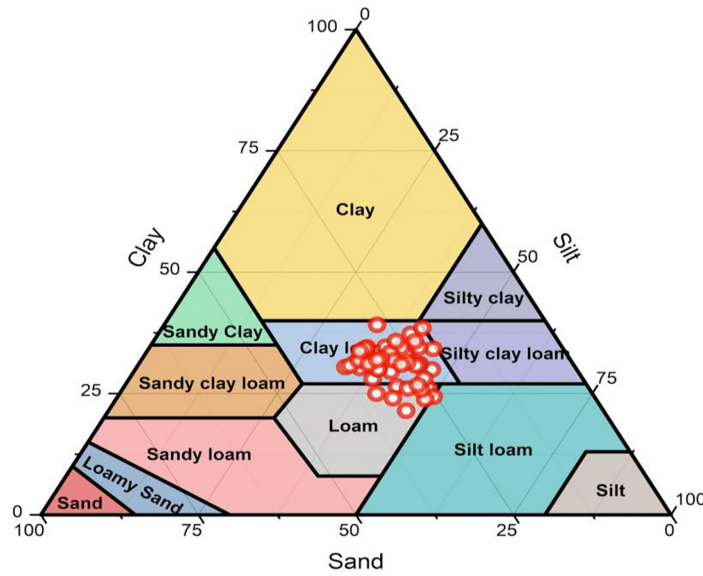


Figure 2. Soil textural class distribution on the USDA textural triangle

silt, and clay with 14.17%, 11.49%, and 12.49%, respectively, indicating a similar soil series derived from the same parent material and has undergone natural development as well as potential influence by human activities. Furthermore, the relationship between the soil pH and EC and the textural classes presented variability, as shown in Figure 3. Clay loam soils tend to have a wider pH than the loamy soils, while both soil types have a wider EC range. The variation in pH and EC is mostly due to the diverse soil management strategies implemented.

The skewness and kurtosis values were relatively small (<1) except for EC. Soil pH and EC were positively skewed and both properties have positive kurtosis values, while sand and clay have negative skewness and kurtosis values. Silt has positive skewness and a negative kurtosis. If the

data are not significantly skewed, the ordinary kriging predictor performs better. A skewness and kurtosis value close to zero suggests a normal distribution [Vieira et al., 2002]. The soil EC is not normally distributed at 0.05 significant level according to the KS test. Box-Cox transformation was appropriate to normalize the soil EC. It is normal for some soil data not to follow a normal distribution [McGrath and Zhang, 2003]. However, kriging approaches are useful when normal distribution is observed [Johnston et al., 2001; Zhang, 2006]. Data normalization improves data stationarity and reduces outliers.

Figure 4 illustrates the Pearson correlation coefficients of the soil parameters. EC, clay, and silt significantly correlate with soil pH while clay and silt are significantly correlated with EC. Particle size fractions (sand, silt, and clay)

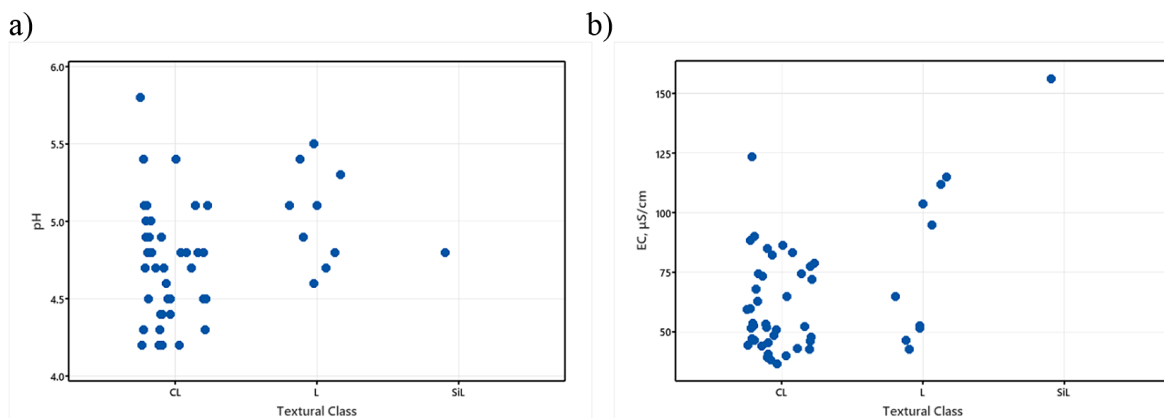


Figure 3. Individual value plot of (a) pH and (b) EC grouped by textural classes (CL = clay loam, L = loam, SiL = silt loam)

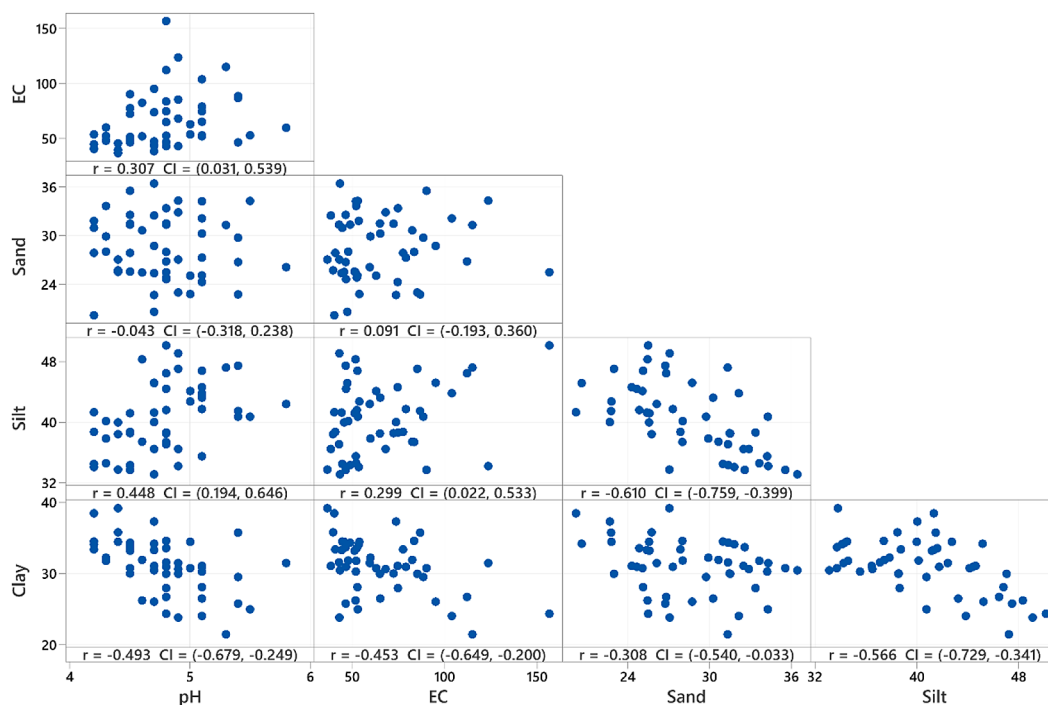


Figure 4. Pearson correlation matrix plot of pH, EC, sand, silt, and clay

are significantly correlated. Regarding the level of correlation among properties, pH has a moderate correlation (positive) with EC ($r = 0.307$) and silt ($r = 0.448$). Clay has a moderate correlation (negative) with pH ($r = -0.493$) and EC ($r = -0.453$). Furthermore, EC and silt have a weak correlation (positive) ($r = 0.299$). In terms of the particle fractions, silt has a strong correlation (negative) with clay ($r = -0.566$) and sand ($r = -0.610$) while clay has a weak correlation (negative) with sand ($r = -0.308$). The relationship between the three fractions of soil particles is inversely proportional, as their combined total equals 100%.

Geostatistics and spatial variability mapping

The optimal model was selected for the ordinary kriging of the soil properties. Table 2 and

Figure 5 show the best-fit semivariogram models. Clay content has no nugget effect following the spherical model. Nugget of the other soil parameters can be attributed to both inherent measurement errors or variations at smaller distances than the sample interval [Oliver and Webster, 2014]. The observed sill values, the value of the semivariogram at which the model becomes flat, were relatively small.

The maximum distance at which a variable no longer exhibits spatial dependence is denoted by the range. The range values for soil pH, EC, and particle size fractions were between 56.20 to 193.86 m. A low range value indicates that soil properties are primarily influenced by their immediate neighboring values, and less influenced by values at farther distances [Mcbratney and Webster, 1983, Lopez-Granados et al., 2002].

Table 2. Best-fitted semivariogram model parameters of the soil variables

Parameter	Model	Nugget (C_0)	Partial Sill (C_1)	Sill, ($C_0 + C_1$)	Nugget/sill ratio ^a (%)	DSD ^b	Range (m)
pH	Spherical	0.0645	0.0935	0.1580	40.82	Moderate	193.86
EC ^c	Exponential	5.46×10^{-6}	2.16×10^{-5}	2.71×10^{-5}	20.15	Strong	56.20
Sand	Spherical	9.4686	0.7250	10.1936	92.89	Weak	70.58
Silt	Spherical	8.7941	6.9286	15.7227	55.93	Moderate	118.42
Clay	Spherical	0.0000	12.9736	12.9736	0.00	Strong	57.95

Note: ^aNugget/sill ratio(%) = $C_0 / (C_0 + C_1) \times 100$; ^bDegree of spatial dependence (DSD); strong <25%, moderate 25–75% and weak > 75%, ^cBox-Cox transformed

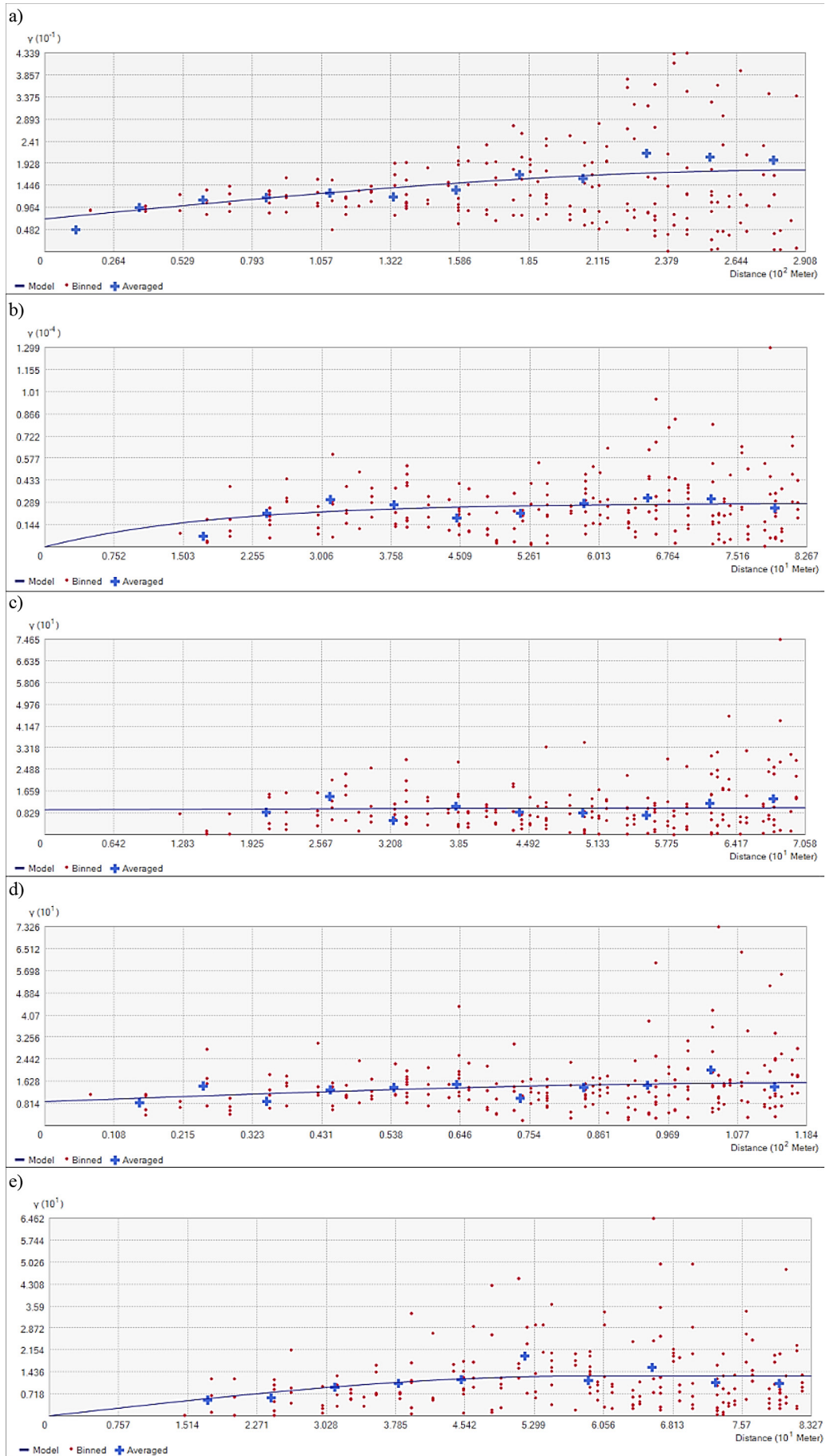


Figure 5. Fitted semivariograms of (a) pH, (b) EC, (c) sand, (d) silt, and (e) clay

Spatial autocorrelation extends beyond the distance covered by the sampling interval (<50 m). Therefore, the method of sampling strategy is suitable for this investigation, and the interpolated map is anticipated to be effective in reflecting the underlying spatial variation.

The nugget/sill ratio (%) values of pH, EC, sand, silt, and clay were 40.82, 20.15, 92.89, 55.93, and 0.00%, respectively. The nugget/sill ratio was utilized to categorize the DSD exhibited by soil parameters. The strong spatial dependency of EC and clay suggests that the random elements less likely affected its spatial distribution. Soil pH and silt were observed to have a moderate spatial dependence while sand has a weak spatial dependence.

Cross-validation

The models' performances were evaluated by analyzing their prediction errors. Prediction errors of the best-suited methods are shown in Table 3. Cross-validation estimates the model using all available data. The algorithm individually removes each data from sampling locations and guesses the corresponding data value using the remaining data. This was done to identify the semivariogram model that would generate the most accurate predictions. By analyzing the estimated prediction errors, it was evaluated how well the model captured the spatial variation of each variable, ultimately determining its suitability for mapping these properties. To ensure model reliability, the ME and MSE values should approach zero, while both ASE and RMSE values should be small and close to each other, and the RMSSE value should approximate one [Johnston et al., 2001]. It was determined that the best model for pH, sand, silt, and clay was spherical while the best model for EC was exponential.

After choosing the most suitable theoretical models and their corresponding semivariogram parameters, spatial variability maps were generated (Fig. 6). According to the soil pH map, the NE part exhibited higher pH levels in comparison to other

areas depicted on the map. This area is being regularly used for organic trials, and the addition of organic fertilizers and lime applications have contributed to the improvement of soil pH. The EC within the area is quite varied but these values are very low (< 4000 $\mu\text{S}\cdot\text{cm}^{-1}$), indicating that the area has very low soluble salt content. In terms of soil texture fractions, sand is high from NW to W and low in the S. Silt content is increasing from W to E while the clay content is higher in the center of the area and some portions of the N and S and there is a decrease in W and E areas. Even within the same soil series, differences in management can lead to variations in soil properties. These maps are valuable for precision farming and tailored management strategies.

Delineation of management zones

Figure 7 shows the location and size of the three distinct management zones (MZ1, MZ2, and MZ3) identified. A considerable portion (82.10%) was classified as MZ1 with weakly acidic (pH 4.5–6.5) clay loam soil. To ensure that soil pH remains suitable for optimal growth of crops, periodic lime application is recommended. This will help neutralize acidity and improve nutrient availability. A small fraction (15.11%) was classified as MZ2 with weakly acidic loam soil. Similar to MZ1, maintaining pH within the optimal range through lime application is essential for MZ2. Certain vegetables, such as carrots, lettuce, and potatoes thrive in loamy soils due to their good drainage and nutrient availability. The smallest zone was MZ3 (2.79%) with highly acidic (pH > 4.5) loam soil. Given the highly acidic nature of this zone, more frequent and intensive lime application is necessary to raise the pH above 5.0. Acid-tolerant crops may be suitable. However, if pH is adequately corrected, a wider range of crops can be considered. Furthermore, enhanced fertilization may be required, as less nutrients become less available in highly acidic soils.

Table 3. Cross-validation parameters of the best-fit models

Parameter	Model	Prediction errors				
		ME	RMSE	MSE	RMSSE	ASE
pH	Spherical	-0.0022	0.3394	-0.0114	1.0734	0.3147
EC	Exponential	-1.7257	25.5141	-0.1509	1.1556	26.9481
Sand	Spherical	-0.0629	3.3065	-0.0194	0.97516	3.3754
Silt	Spherical	-0.0336	3.9611	-0.0106	1.0782	3.6369
Clay	Spherical	-0.0486	3.4081	-0.0084	1.0013	3.3551

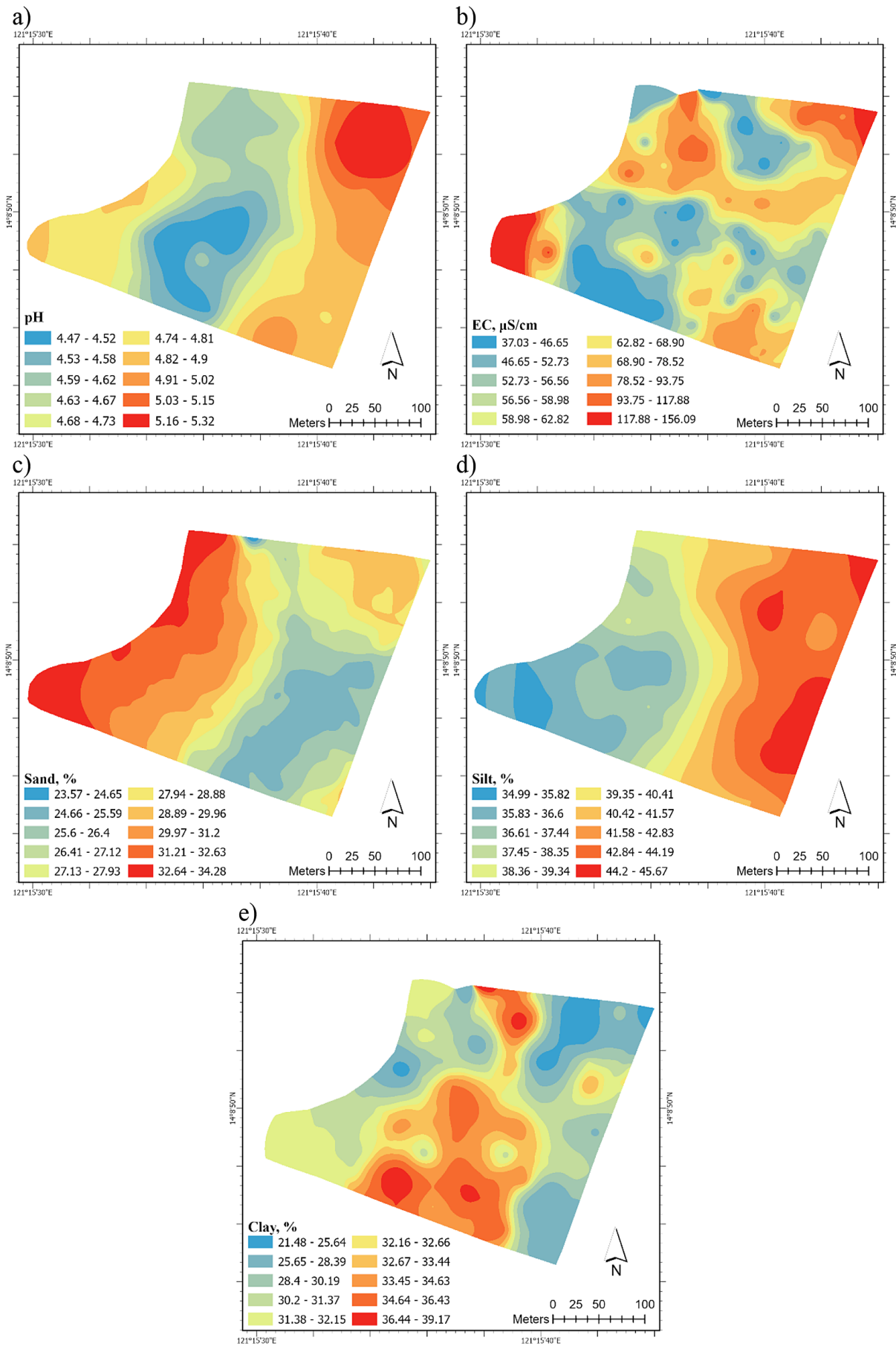


Figure 6. Spatial distribution of (a) pH, (b) EC, (c) sand, (d) silt, and (e) clay in the study area

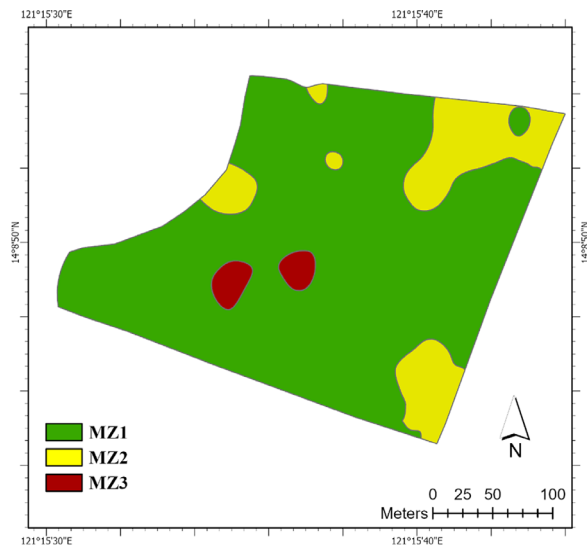


Figure 7. Delineation of management zones in the study area

CONCLUSIONS

The mapping and assessment of soil properties as well as delineation of management zones are both important aspects of land management. This study investigated the within-field spatial variation of soil pH, EC, sand, silt, and clay content using ordinary kriging. Subsequently, the resulting maps were used to define optimal management zones. The findings indicate that the area has predominantly acidic, medium-textured soil with low EC. Descriptive statistics show the low pH and soil texture variability while EC has high variability. The nugget/sill ratio ranges from 0% to 92.89%. Clay and EC exhibited strong spatial dependence, indicating the dominant influence of inherent soil-forming processes. The soil pH and silt content showed moderate dependence, indicating the combined effects of intrinsic and extrinsic influences like parent material and management practices, respectively. Sand, with weak dependence, appeared most affected by random elements and external management. Leveraging these spatial patterns and using the interpolated maps, three management zones (MZ1, MZ2, and MZ3) were delineated covering 82.10%, 15.11%, and 2.79% of the area, respectively. Overall, lime application is recommended due to low soil pH. However, a more frequent and intensive lime application is advised for MZ3 due to its highly acidic soil condition. The maps may be utilized to provide optimal management strategies within the area. The findings highlight a practical

approach to use interpolated maps for delineating management zones. Further studies may examine the potential of incorporating remotely sensed data to possibly improve the identification of management zones.

REFERENCES

1. AbdelRahman, M.A., Zakarya, Y.M., Metwaly, M.M., Koubouris, G. 2020. Deciphering soil spatial variability through geostatistics and interpolation techniques. *Sustainability*, 13(1), 194. <https://doi.org/10.3390/su13010194>
2. Amirinejad, A.A., Kamble, K., Aggarwal, P., Chakraborty, D., Pradhan, S., Mittal, R.B. 2011. Assessment and mapping of spatial variation of soil physical health in a farm. *Geoderma*, 160(3–4), 292–303. <https://doi.org/10.1016/j.geoderma.2010.09.021>
3. Buol, S.W., Southard, R.J., Graham, R.C., McDaniel, P.A. 2011. Soil genesis and classification. <https://doi.org/10.1002/9780470960622>
4. Cambardella, C.A., Moorman, T.B., Novak, J.M., Parkin, T.B., Karlen, D.L., Turco, R.F., Konopka, A.E. 1994. Field-scale variability of soil properties in central Iowa soils. *Soil Science Society of America Journal*, 58(5), 1501–1511. <https://doi.org/10.2136/sssaj1994.03615995005800050033x>
5. Carating, R.B., Galanta, R.G. and Bacatio, C.D. 2014. The soils of the Philippines. <https://doi.org/10.1007/978-94-017-8682-9>
6. Damian, J.M., Santi, A.L., Fornari, M., Da Ros, C.O., Eschner, V.L. 2017. Monitoring variability in cash-crop yield caused by previous cultivation of a cover crop under a no-tillage system. *Computers and Electronics in Agriculture*, 142, 607–621. <https://doi.org/10.1016/j.compag.2017.11.006>
7. Davatgar, N., Neishabouri, M.R., Sepaskhah, A.R. 2012. Delineation of site specific nutrient management zones for a paddy cultivated area based on soil fertility using fuzzy clustering. *Geoderma*, 173–174, 111–118. <https://doi.org/10.1016/j.geoderma.2011.12.005>
8. Delbari, M., Afrasiab, P., Gharabaghi, B., Amiri, M., Salehian, A. 2019. Spatial variability analysis and mapping of soil physical and chemical attributes in a salt-affected soil. *Arabian Journal of Geosciences*, 12, 1–18. <https://doi.org/10.1007/s12517-018-4207-x>
9. Desavathu, R.N., Nadipena, A.R., Peddada, J.R. 2018. Assessment of soil fertility status in Paderu Mandal, Visakhapatnam district of Andhra Pradesh through Geospatial techniques. *The Egyptian Journal of Remote Sensing and Space Science*, 21(1), 73–81. <https://doi.org/10.1016/j.ejrs.2017.01.006>
10. FAO. 2021. Standard operating procedure for soil

- electrical conductivity, soil/water, 1:5.
11. FAOb. 2021. Standard operating procedure for soil pH determination.
 12. Fu, W., Tunney, H., Zhang, C. 2010. Spatial variation of soil nutrients in a dairy farm and its implications for site-specific fertilizer application. *Soil and Tillage Research*, 106(2), 185–193. <https://doi.org/10.1016/j.still.2009.12.001>
 13. Fraisse, C.W., Sudduth, K.A., Kitchen, N.R. 2001. Delineation of Site-Specific Management Zones by Unsupervised Classification of Topographic Attributes and Soil Electrical Conductivity. *Transactions of the ASABE*, 44, 155–166.
 14. Gili, A., Álvarez, C., Bagnato, R., Noellemeyer, E. 2017. Comparison of three methods for delineating management zones for site-specific crop management. *Computers and Electronics in Agriculture*, 139, 213–223. <https://doi.org/10.1016/j.compag.2017.05.022>
 15. Georgi, C., Spengler, D., Itzerott, S., Kleinschmit, B. 2017. Automatic delineation algorithm for site-specific management zones based on satellite remote sensing data. *Precision Agriculture*, 19(4), 684–707. <https://doi.org/10.1007/s11119-017-9549-y>
 16. He, Y., Hu, K.L., Huang, Y.F., Li, B.G., Chen, D.L. 2010. Analysis of the anisotropic spatial variability and three-dimensional computer simulation of agricultural soil bulk density in an alluvial plain of north China. *Mathematical and Computer Modelling*, 51(11–12), 1351–1356. <https://doi.org/10.1016/j.mcm.2009.11.011>
 17. Heijting, S., De Bruin, S., Bregt, A.K. 2010. The arable farmer as the assessor of within-field soil variation. *Precision Agriculture*, 12(4), 488–507. <https://doi.org/10.1007/s11119-010-9197-y>
 18. Jin, Z., Prasad, R., Shriver, J., Zhuang, Q. 2016. Crop model- and satellite imagery-based recommendation tool for variable rate N fertilizer application for the US Corn system. *Precision Agriculture*, 18(5), 779–800. <https://doi.org/10.1007/s11119-016-9488-z>
 19. Johnston, K., Ver Hoef, J.M., Krivoruchko, K., Lucas, N. 2001. Using ArcGIS geostatistical analyst.
 20. Jones, J.B. 2001. Laboratory guide for conducting soil tests and plant analysis. CRC press. <https://doi.org/10.1201/9781420025293>
 21. Júnior, V.V., Carvalho, M., Dafonte, J., Freddi, O., Vázquez, E.V., Ingaramo, O. 2006. Spatial variability of soil water content and mechanical resistance of Brazilian ferralsol. *Soil & Tillage Research*, 85(1–2), 166–177. <https://doi.org/10.1016/j.still.2005.01.018>
 22. Khan, M.Z., Islam, M.R., Salam, A.B.A., Ray, T. 2021. Spatial variability and geostatistical analysis of soil properties in the diversified cropping regions of Bangladesh using geographic information system techniques. *Applied and Environmental Soil Science*, 1–19. <https://doi.org/10.1155/2021/6639180>
 23. Koch, B., Khosla, R., Frasier, W.M., Westfall, D.G., Inman, D. 2004. Economic feasibility of variable-rate nitrogen application utilizing site-specific management zones. *Agronomy Journal*, 96(6), 1572–1580. <https://doi.org/10.2134/agronj2004.1572>
 24. Laekemariam, F., Kibret, K., Mamo, T., Shiferaw, H. 2018. Accounting spatial variability of soil properties and mapping fertilizer types using geostatistics in southern Ethiopia. *Communications in Soil Science and Plant Analysis*, 49(1), 124–137. <https://doi.org/10.1080/00103624.2017.1421656>
 25. Leroux, C. and Tisseyre, B. 2018. How to measure and report within-field variability: a review of common indicators and their sensitivity. *Precision Agriculture*, 20(3), 562–590. <https://doi.org/10.1007/s11119-018-9598-x>
 26. Li, L., Zhao, Z., Peng, Z., Qin, S. 2013. Soil spatial variability and interpolation method based on GIS in large scale. *Guizhou Agricultural Sciences*, 8, 195–199. <https://doi.org/10.1016/j.jssas.2016.02.001>
 27. Liu, C.L., Wu, Y.Z., Liu, Q.J. 2015. Effects of land use on spatial patterns of soil properties in a rocky mountain area of Northern China. *Arabian Journal of Geosciences*, 8, 1181–1194. <https://doi.org/10.1007/s12517-013-1233-6>
 28. López-Granados, F., Jurado-Expósito, M., Atenciano, S., García-Ferrer, A., Sánchez de la Orden, M., García-Torres, L. 2002. Spatial variability of agricultural soil parameters in southern Spain. *Plant and Soil*, 246, 97–105. <https://doi.org/10.1023/A:1021568415380>
 29. Losser, T., Li, L., Piltner, R. 2014. A spatiotemporal interpolation method using radial basis functions for geospatiotemporal big data. In: *Fifth International Conference on Computing for Geospatial Research and Application*. IEEE. <https://doi.org/10.1109/COM.Geo.2014.15>
 30. McBratney, A.B., and Webster, R. 1983. How many observations are needed for regional estimation of soil properties? *Soil Science*, 135(3), 177–183.
 31. McGrath, D., and Zhang, C. 2003. Spatial distribution of soil organic carbon concentrations in grassland of Ireland. *Applied Geochemistry*, 18(10), 1629–1639. [https://doi.org/10.1016/S0883-2927\(03\)00045-3](https://doi.org/10.1016/S0883-2927(03)00045-3)
 32. Moral, F., Terrón, J., Da Silva, J.M. 2010. Delineation of management zones using mobile measurements of soil apparent electrical conductivity and multivariate geostatistical techniques. *Soil & Tillage Research*, 106(2), 335–343. <https://doi.org/10.1016/j.still.2009.12.002>
 33. Nolan, S.C., Goddard, T.W., Lohstraeter, G., Coen, G.M., Robert, P.C., Rust, R.H., Larson, W.E. 2000. Assessing managements units on rolling topography. *Proceedings of the 5th International Conference on Precision Agriculture*, Bloomington, Minnesota, USA, 16–19 July, 2000: 1–12
 34. Oliver, M.A., and Webster, R. 2014. A tutorial guide

- to geostatistics: Computing and modelling variograms and kriging. *Catena*, 113, 56–69. <https://doi.org/10.1016/j.catena.2013.09.006>
35. Pardo-Igúzquiza, E., and Dowd, P.A. 2013. Comparison of inference methods for estimating semi-variogram model parameters and their uncertainty: The case of small data sets. *Computers and Geosciences*, 50, 154–164. <https://doi.org/10.1016/j.cageo.2012.06.002>
 36. Pereira, P., Brevik, E.C., Cerdà, A., Úbeda, X., Novara, A., Francos, M., Comino, J.R., Bogunovic, I. and Khaleedian, Y. 2017. Mapping ash CaCO₃, pH, and extractable elements using principal component analysis. In: *Soil Mapping and Process Modeling for Sustainable Land Use Management*. <https://doi.org/10.1016/B978-0-12-805200-6.00010-4>
 37. Reza, S.K., Baruah, U., Sarkar, D., Singh, S.K. 2016. Spatial variability of soil properties using geostatistical method: A case study of lower Brahmaputra plains, India. *Arabian Journal of Geosciences*, 9, 1–8. <https://doi.org/10.1007/s12517-016-2474-y>
 38. Reza, S.K., Sarkar, D., Baruah, U., Das, T.H. 2010. Evaluation and comparison of ordinary kriging and inverse distance weighting methods for prediction of spatial variability of some chemical parameters of Dhalai district, Tripura. *Agropedology*, 20(1), 38–48.
 39. Richards L.A. 1954. *Diagnosis and Improvement of Saline and Alkaline Soils*. Handbook No. 60. US Department of Agriculture, Washington.
 40. Sadras, V. and Bongiovanni, R. 2004. Use of Lorenz curves and Gini coefficients to assess yield inequality within paddocks. *Field Crops Research*, 90(2–3), 303–310. <https://doi.org/10.1016/j.fcr.2004.04.003>
 41. Santi, A., Amado, T., Eitelwein, M., Cherubin M., Silva, R., Ros, C. 2013. Definição de zonas de produtividade em áreas manejadas com agricultura de precisão. *Agrária*, 8(3), 510–515. <https://doi.org/10.5039/agraria.v8i3a2489>
 42. Shi, W., Liu, J., Du, Z., Song, Y., Chen, C., Yue, T. 2009. Surface modelling of soil pH. *Geoderma*, 150(1–2), 113–119. <https://doi.org/10.1016/j.geoderma.2009.01.020>
 43. Shukla, A.K., Behera, S.K., Lenka, N.K., Tiwari, P.K., Prakash, C., Malik, R.S., Sinha, N.K., Singh, V.K., Patra, A.K., Chaudhary, S.K. 2016. Spatial variability of soil micronutrients in the intensively cultivated Trans-Gangetic Plains of India. *Soil and Tillage Research*, 163, 282–289. <https://doi.org/10.1016/j.still.2016.07.004>
 44. Tripathi, R., Nayak, A., Shahid, M., Lal, B., Gautam, P., Raja, R., Mohanty, S., Kumar, A., Panda, B., Sahoo, R. 2015. Delineation of soil management zones for a rice cultivated area in eastern India using fuzzy clustering. *Catena*, 133, 128–136. <https://doi.org/10.1016/j.catena.2015.05.009>
 45. Vasu, D., Singh, S.K., Sahu, N., Tiwary, P., Chandran, P., Duraisami, V.P., Ramamurthy, V., Lalitha, M., Kalaiselvi, B. 2017. Assessment of spatial variability of soil properties using geospatial techniques for farm level nutrient management. *Soil and Tillage Research*, 169, 25–34. <https://doi.org/10.1016/j.still.2017.01.006>
 46. Vieira, S.R., Millete, J., Topp, G.C., Reynolds, W.D. 2002. *Handbook for geostatistical analysis of variability in soil and climate data*. Topics in Soil Science, 2, 1–45.
 47. Vrindts, E., Mouazen, A., Reyniers, M., Maertens, K., Maleki, Ramon, H., De Baerdemaeker, J. 2005. Management zones based on correlation between soil compaction, yield and crop data. *Biosystems Engineering*, 92(4), 419–428. <https://doi.org/10.1016/j.biosystemseng.2005.08.010>
 48. Webster, R., and Oliver, M.A. 2007. *Geostatistics for environmental scientists*. <https://doi.org/10.1002/9780470517277>
 49. Wilding, L.P. 1985. Spatial variability: its documentation, accommodation and implication to soil surveys.
 50. Xin-Zhong, W., Guo-Shun, L., Hong-Chao, H., Zhen-Hai, W., Qing-Hua, L., Xu-Feng, L., Wei-Hong, H., Yan-Tao, L. 2009. Determination of management zones for a tobacco field based on soil fertility. *Computers and Electronics in Agriculture*, 65(2), 168–175. <https://doi.org/10.1016/j.compag.2008.08.008>
 51. Yang, Z., Chen, P., Liu, J., Yu, K., Liao, X., You, H., Miao, L. 2012. Spatial interpolation of forest soil nutrients based on Kriging method. *Journal of Fujian Agriculture and Forestry University (Natural Science Edition)*, 41(3), 296–300.
 52. Zhang, C. 2006. Using multivariate analyses and GIS to identify pollutants and their spatial patterns in urban soils in Galway, Ireland. *Environmental Pollution*, 142(3), 501–511. <https://doi.org/10.1016/j.envpol.2005.10.028>